

Towards Imitation Learning in Real World Unstructured Social Mini-Games in Pedestrian Crowds

Rohan Chandra¹, Haresh Karnan¹, Negar Mehr², Peter Stone^{1,3}, Joydeep Biswas¹
{rchandra, haresh.miriyala, pstone, joydeepb}@utexas.edu, negar@berkeley.edu
Dept. of Computer Science at The University of Texas at Austin¹
Dept. of Mechanical Engineering at the University of California, Berkeley²
Sony AI, USA³

Abstract—Imitation Learning (IL) strategies are used to generate policies for robot motion planning and navigation by learning from human trajectories. Recently, there has been a lot of excitement in applying IL in social interactions arising in urban environments such as university campuses, restaurants, grocery stores, and hospitals. However, obtaining numerous expert demonstrations in social settings might be expensive, risky, or even impossible. Current approaches therefore, focus only on simulated social interaction scenarios. This raises the question: *How can a robot learn to imitate an expert demonstrator from real world multi-agent social interaction scenarios?* It remains unknown which, if any, IL methods perform well and what assumptions they require.

We benchmark representative IL methods in real world social interaction scenarios on a motion planning task, using a novel pedestrian intersection dataset collected at the University of Texas at Austin campus. Our evaluation reveals two key findings: first, learning multi-agent cost functions is required for learning the diverse behavior modes of agents in tightly coupled interactions and second, conditioning the training of IL methods on partial state information or providing global information in simulation can improve imitation learning, especially in real world social interaction scenarios.

I. INTRODUCTION

Robot navigation in densely populated human environments has garnered significant attention. Of particular interest are tightly coupled social interactions between pedestrians, scooters, and vehicles in geometrically constrained scenarios such as intersections, hallways, narrow gaps, etc. These scenarios, which we refer to as *Social Mini-Games* or SMGs [1], occur both in outdoor settings [2], [3], [4], [5] as well as indoor spaces like restaurants, grocery stores, hospitals, and university campuses [6], [7], [8], [9], [10], [11]. Despite some success, deploying robots in SMGs in a socially compliant manner, such as yielding to a pedestrian, is challenging as social compliance requires predicting and reacting to humans' intents as well as projecting their own [12], [13]. Since humans are most adept at navigating SMGs in a socially compliant way, imitation learning (IL) has been instrumental in social robot navigation [6] where robot navigation policies are learned by mimicking human trajectories.

This work has taken place in the Autonomous Mobile Robotics Laboratory (AMRL) as well as the Learning Agents Research Group (LARG) at UT Austin. AMRL research is supported in part by NSF (CAREER-2046955, IIS-1954778, CCF-2006404, OIA-2219236, DGE-2125858, CCF-2319471), ARO (W911NF-23-2-0004), Amazon, and JP Morgan. LARG research is supported in part by NSF (FAIN-2019844, NRT-2125858), ONR (N00014-18-2243), ARO (E2061621), Bosch, Lockheed Martin, and UT Austin's Good Systems grand challenge. Peter Stone serves as the Executive Director of Sony AI America and receives financial compensation for this work. The terms of this arrangement have been reviewed and approved by the University of Texas at Austin in accordance with its policy on objectivity in research. Negar Mehr is supported by NSF CCF-2211542.

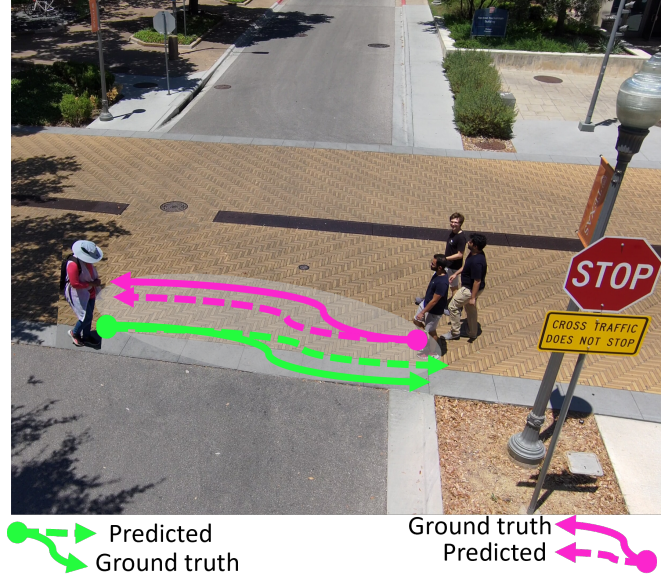


Fig. 1: Visualizing the imitation learning problem for motion planning at the Speedway intersection on the University of Texas at Austin campus. We refer to such interactions as social mini-games.

However, acquiring large volumes of expert demonstration data in urban settings is not only resource-intensive but can also be challenging due to safety and privacy concerns. This constraint has limited the state-of-the-art approaches to work primarily in simulated environments leading us to ask: *Can imitation learning be used to learn robot navigation policies for real world SMGs?*

This research sets out to bridge this knowledge gap by studying the strengths, limitations, and the various assumptions made by various IL methods in real world SMGs. Using a novel dataset collected on the University of Texas at Austin campus, we benchmark and evaluate the comparative performance of these methods in pedestrian-rich contexts. Through this study, we aim to guide the selection of appropriate IL techniques for motion planning in large pedestrian crowds, ensuring that robots can navigate shared spaces safely and with social awareness.

The methods benchmarked in this study follow the taxonomy laid out in seminal surveys on imitation learning [14], [15] that split IL methods broadly into behavior cloning (BC), inverse reinforcement learning (IRL), and generative methods. We pick, and compare, representative methods from

each class. For instance, the representative method for IRL is the original Maximum Entropy IRL (MaxEnt IRL) algorithm proposed by Ziebart et al. [16].

Main contributions: In this work,

- 1) We present the first study of IL methods, such as behavior cloning, generative models, and inverse reinforcement learning, applied to motion planning in real pedestrian crowds. Our evaluation reveals two key findings: (i), learning multi-agent cost functions is required for learning the diverse behavior modes of agents in tightly coupled interactions and (ii) conditioning the training of behavior cloning on partial state information or providing global information in simulation can improve imitation learning, especially in real world social interaction scenarios.
- 2) We release a new dataset¹ collected on the campus of the University of Texas at Austin. It consists of 3 hours of trajectory data collected at a busy intersection consisting of positions, velocity, heading angle, and class ids of pedestrians. Our dataset primarily consists of tightly coupled agent interactions that are rarely found in existing autonomous driving or urban pedestrian datasets.

II. IMITATION LEARNING: BACKGROUND

IL represents a machine learning paradigm where an autonomous agent strives to learn a behavior by emulating an expert’s demonstrations. Typically, the demonstrations comprise state-action pairs, generated by an expert policy during real-world execution. Addressing the imitation learning problem has led to three major approaches, namely, Behavior Cloning (BC) [17], [18], [19], which involves direct learning of an imitative policy through supervised learning, Inverse Reinforcement Learning (IRL) [20], [21], [22], wherein a reward function is first inferred from the demonstrations, subsequently used to guide policy learning via Reinforcement Learning (RL) [23], and generative models [24], [25], [26]. We refer the reader to Zhang et al. [15] for a more comprehensive background on IL.

A. Behavior Cloning

Given a sequence of tuples containing state-action pairs in the expert demonstration, Behavior Cloning (BC) employs a supervised learning approach to learn the imitator’s policy mapping from states to actions [27], [28]. Despite its relative ease of implementation and ability to scale and perform effectively in a large-scale data regime, BC is known to suffer from a compounding error issue [29]. This problem typically arises due to a slight deviation from the expert trajectory leading to drastic errors over time, a characteristic feature of BC. Regardless, the primary focus of this work is on offline imitation learning techniques, which are uniquely designed to operate with a static, comprehensive dataset of expert demonstrations. These methods hold considerable promise for enhancing efficiency and reproducibility in complex tasks, particularly in multi-agent human motion prediction.

¹<https://amrl.cs.utexas.edu/imitation-learning-benchmark.html>

B. Inverse Reinforcement Learning

While traditional IRL methods achieved success, they were primarily designed for discrete state and action spaces. In contrast, Levine et al. investigated maximum entropy cost inference for systems with continuous state and action spaces [30]. A common assumption in these studies involved parameterizing the agent’s cost function as a weighted sum of known features. This assumption was relaxed in Finn et al.’s work [31], where the underlying cost function was learned using a neural network within the maximum-entropy framework. In the context of bilevel optimization, works like [32], [33] focused on inferring an agent’s cost function by optimizing the estimation error of system trajectories or the likelihood of demonstrations.

While previous approaches focused on learning in the single-agent regime, multi-Agent IRL has been extensively studied in various settings. Adversarial machine learning techniques were employed for high-dimensional state and action spaces [34], and generative adversarial imitation learning was extended to the multi-agent setting [35]. Additionally, the problem has been approached as an estimation task [36], [37], and linear quadratic games were considered with known equilibrium strategies [38], [39]. The maximum entropy IRL [40] framework was introduced to accommodate bounded rationality and noisy human demonstrations. These studies highlight the diverse and evolving landscape of multi-agent IRL.

C. Generative Models

In a recent development, a novel category of imitation learning algorithms known as Adversarial Imitation Learning (AIL) [24], [25], [26] has emerged. AIL introduces an intriguing adversarial setup akin to the concept of Generative Adversarial Networks (GANs). Here, the agent employs two neural networks: a discriminator, responsible for distinguishing expert experiences from the imitator’s, and a generator network that models the imitator’s policy, mimicking the expert demonstrations. Among the pioneering AIL algorithms stands out Generative Adversarial Imitation Learning (GAIL) [24], showcasing remarkable ability in replicating expert behavior. GAIL directly extracts a policy from an agent’s demonstrations, similar to reinforcement learning following maximum entropy IRL.

However, a shared drawback among these algorithms is their underlying assumption of having access to the expert’s action data during the demonstration phase, which may not be readily available in all practical scenarios [41]. Additionally, these methods learn from a single agent in isolation.

III. PROBLEM FORMULATION

We define a game, $G := \langle k, \mathcal{X}, \mathcal{T}, \{\mathcal{U}^i\}, \{\mathcal{J}^i\} \rangle$, where k denotes the number of agents. Hereafter, i will refer to the index of an agent and appear as a superscript whereas t will refer to the current time-step and appear as a subscript. The general state space \mathcal{X} (e.g. SE(2), SE(3), etc.) is continuous; the i^{th} agent at time t has a state $x_t^i \in \mathcal{X}^i$. Over a finite horizon T , each agent starts from $x_0^i \in \mathcal{X}^i$ and reaches a goal state $x_T^i \in \mathcal{X}^i$. An agent’s transition function is a mapping, $\mathcal{T}^i : \mathcal{X} \times \mathcal{U}^i \rightarrow \mathcal{X}$, where $u_t^i \in \mathcal{U}^i$ is the continuous control space for agent i . A discrete trajectory is specified by the sequence $\Gamma^i = (x_0^i, u_0^i, x_1^i, u_1^i, \dots, x_{T-1}^i, u_{T-1}^i, x_T^i)$. Each

agent has a parameterized running cost $\mathcal{J}^i : \mathcal{X} \times \mathbf{U} \rightarrow \mathbb{R}$ where $\mathbf{U} = \mathcal{U}^1 \times \mathcal{U}^2 \times \dots \times \mathcal{U}^k$. The cost \mathcal{J}^i acts on joint state x_t and control $\mathbf{u}_t \in \mathbf{U}$ at each time step measuring the distances between agents, deviation from the reference path, and the change in the control input. Each agent i follows a stochastic decentralized policy $\mathcal{F}_{\theta^i}^i : \mathcal{X} \rightarrow \mathcal{U}^i$, which captures the probability of agent i selecting action u_t^i at time t , given that the system is in state x_t . The parameters for the policy \mathcal{F}^i are represented by θ^i , which may correspond to weights of a neural network or coefficients in a weighted linear function. We assume that we are provided with a dataset $\widehat{\mathcal{D}} = \{\widehat{\Gamma}^{1:k}\}_N$ that consists of N expert demonstration trajectories, $\widehat{\Gamma}^i$ for each agent i . Further, we let $\mathcal{D}_{\theta^i} = \{\Gamma_{\theta^i}^{1:k}\}_M$ denote the dataset of M trajectories for each agent generated by the policy $\mathcal{F}_{\theta^i}^i$ parameterized by θ^i (in the case of IRL, $\mathcal{F}_{\theta^i}^i$ implies the reward function is parameterized by θ^i). Our problem statement is then,

Problem 1. Find $\theta^{i,*}$ for $i \in [1, k]$ that minimizes

$$\left\| \mathbb{E}_{\widehat{\Gamma}^i, \Gamma_{\theta^i}^i \sim \widehat{\mathcal{D}}, \mathcal{D}_{\theta^i}} \Psi^i \left(\Gamma_{\theta^i}^i, \widehat{\Gamma}^i \right) \right\| \quad (1)$$

where $\Psi^i \left(\Gamma_{\theta^i}^i, \widehat{\Gamma}^i \right)$ is a generalized discrepancy function that takes on different forms depending on the problem formulation (IRL versus BC, etc.). For instance,

$$\Psi^i \left(\Gamma_{\theta^i}^i, \widehat{\Gamma}^i \right) = \begin{cases} \Phi^i \left(\Gamma_{\theta^i}^i \right) - \Phi^i \left(\widehat{\Gamma}^i \right) & \text{for IRL} \\ \frac{1}{T} \sum_{t=0}^{T-1} \mathcal{F}_{\theta^i}^i \left(x_t \right) - u_t^i & \text{for BC} \end{cases}$$

where $\Phi(\cdot)$ is a feature function that, given a trajectory, returns a vector of features $[\phi_1, \phi_2, \dots, \phi_m]^\top$, averaged across the length of the trajectory, where m refers to the number of distinct features. A simple example of a feature function is the weighted linear sum $\Phi^i \left(\Gamma_{\theta^i}^i \right) = \sum_{t=0}^{T-1} \theta^{i\top} \mathcal{J}^i \left(x_t, \mathbf{u}_t \right)$. In IRL, we want to find parameters θ^i for each agent i such that the feature expectation of the generated trajectories $\widehat{\Gamma}^i$ under the learned cost weights is as close to the empirical feature expectation of the expert demonstrations. Note that we slightly abuse notation and ignore terminal cost at $t = T$.

IV. IL APPROACHES FOR PEDESTRIAN CROWDS

In this section, we discuss the technical approaches underpinning the methods included in our evaluation. Our selection criteria emphasizes both breadth, in terms of different algorithms used and depth, in terms of representing a large set of contemporary approaches. We visually summarize the selection of baselines in Figure 2.

Following the classification of imitation learning in the literature, we discuss behavior cloning (BC), inverse reinforcement learning (IRL), and generative models. Any hybrid models are represented as a separate category. We define a representative algorithm as the best performing method in its category as reported in the literature. For instance, PECNet [42] is the top performing generative method using a conditional variational autoencoder on the ETH/UCY trajectory forecasting benchmark, therefore, it is treated as a representative method for that category.

A. Inverse Reinforcement Learning [43], [40]

Maximum Entropy IRL [43]. In this section, we describe the basic Maximum Entropy Inverse Reinforcement Learning

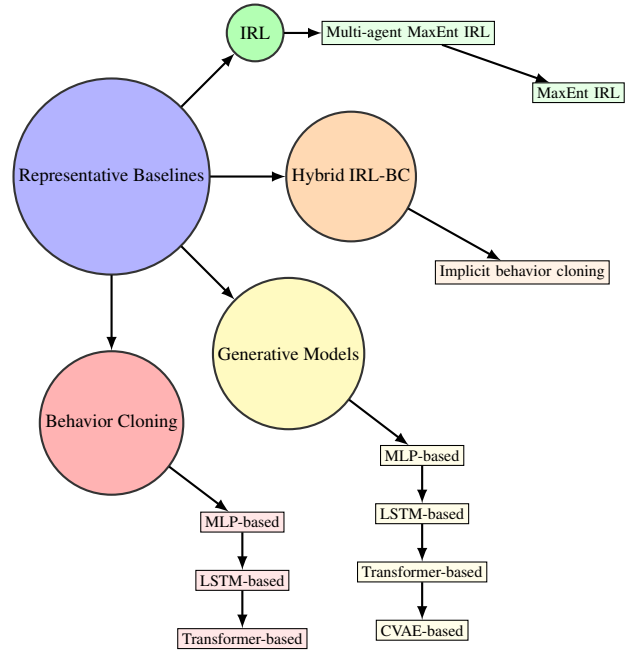


Fig. 2: Representative baselines used for evaluation and benchmarking. The boxed text represents the different algorithms and the underlined text represents the different architectures. Methods listed under the algorithms and architectures indicate usage of the corresponding algorithm or architecture, or both.

(MaxEnt IRL) approach tailored for deriving reward functions from observed expert trajectories [43], [16], followed by highlighting its benefits and the main reasons for its inclusion as a representative baseline.

Traditional Inverse Reinforcement Learning (IRL) seeks to infer a cost function from expert demonstrations [27]. However, multiple cost functions can rationalize the expert’s behavior, leading to inherent ambiguities. MaxEnt IRL addresses this by incorporating the principle of maximum entropy, ensuring that the derived cost function is both unique and maximally uncertain. Given expert trajectories, the probability of a trajectory Γ^i under the MaxEnt framework for agent i is defined as:

$$P \left(\Gamma^i \right) \propto \exp \left(\sum_{t=0}^{T-1} \mathcal{J}^i \left(x_t, u_t^i \right) \right)$$

where $\mathcal{J}^i \left(x_t, u_t^i \right)$ represents the cost for agent i at time t in joint state x_t and taking action u_t^i .

The objective in MaxEnt IRL is to adjust the weights of the cost function such that the expected feature counts under the derived policy match the feature counts of the expert, while also maximizing the entropy of the policy. The cost function is iteratively adjusted, typically using gradient-based methods, to ensure that the expected feature counts from the policy induced by the current reward function align with those from the expert demonstrations. Note that since the MaxEnt IRL algorithm traditionally applies to a single agent, Problem (1) is modified to finding $\theta^{i,*}$ that minimizes

$$\left\| \mathbb{E}_{\Gamma_{\theta^i}^i \sim \mathcal{D}_{\theta^i}} \Phi^i \left(\Gamma_{\theta^i}^i \right) - \mathbb{E}_{\widehat{\Gamma}^i \sim \widehat{\mathcal{D}}} \Phi^i \left(\widehat{\Gamma}^i \right) \right\| \quad (2)$$

There are several reasons why the MaxEnt IRL has been selected as a representative baseline in this study. First, the

maximum entropy principle ensures a unique solution to the reward recovery problem, mitigating ambiguities inherent in traditional IRL. Further, resultant policies are inherently stochastic, capturing a broader range of behaviors and offering robustness in dynamic environments. Finally, MaxEnt IRL can generalize better to unseen states, making it particularly suitable for complex environments like pedestrian crowds [43]. Lastly, in the low data regime, MaxEnt IRL is comparable, if not superior, to many variants that build on top of the base algorithm using deep neural networks.

Multi-agent Maximum-Entropy IRL [40]. In MaxEnt IRL [40], the goal is to learn a cost function that applies either to a single agent or is designed to collectively model a group of individuals. However, individuals in groups behave differently according to their nature. For instance, some individuals might be more risk averse than others, and therefore, are more likely to have a higher reward for collision avoidance. Others might place greater importance on reaching their goals faster and therefore place greater weight for the cost of distance to goal. Therefore, we include the multi-agent MaxEnt IRL framework proposed by Mehr et al. [40].

We assume for simplicity that a pedestrian’s cost is a weighted linear function $\Phi^i(\Gamma_{\theta^i}) = \sum_{t=0}^{T-1} \theta^i \mathcal{J}^i(x_t, \mathbf{u}_t)$ where $\Phi^i(\Gamma_{\theta^i})$ computes the features for agent i with respect to weights θ^i and costs $\mathcal{J}^i(x_t, \mathbf{u}_t)$. In this case, solving Equation (1) reduces to finding $\theta^{i,*}$ for every i such that,

$$\theta^{i,*} = \arg \min_{\theta^i} \left\| \mathbb{E}_{\Gamma_{\theta^i} \sim \mathcal{D}_{\theta^i}} \Phi^i(\Gamma_{\theta^i}) - \mathbb{E}_{\hat{\Gamma}^i \sim \hat{\mathcal{D}}} \Phi^i(\hat{\Gamma}^i) \right\| \quad (3)$$

Equation (3) can be efficiently solved via block coordinate descent [44] where we treat θ as a concatenation of each θ^i , where i then refers to a coordinate. An update to the current cost parameters, θ_{old}^i , of agent i is of the following form,

$$\begin{aligned} \theta_{\text{new}}^i &\leftarrow \theta_{\text{old}}^i - \beta \left(\mathbb{E}_{\Gamma_{\theta_{\text{old}}^i} \sim \mathcal{D}_{\theta_{\text{old}}^i}} \theta_{\text{old}}^i \top \Phi^i(\Gamma_{\theta_{\text{old}}^i}) - \mathbb{E}_{\hat{\Gamma}^i \sim \hat{\mathcal{D}}} \Phi^i(\hat{\Gamma}^i) \right) \\ \theta_{\text{old}}^i &\leftarrow \theta_{\text{new}}^i \end{aligned} \quad (4)$$

where we compute the features for trajectories generated from the new set of cost parameters (θ_{new}^i) and proceed to update the cost parameters for the next agent. We iterate over each agent i and repeat this process until convergence. At each iteration of the update process, each agent i uses its parameterized stochastic policy $\mathcal{F}_{\theta^i}^i(x_t)$ to roll out M trajectories $\{\Gamma^i\}_M$ corresponding to the updated cost parameters (θ_{new}^i). In the case of multi-agent IRL, the policy $\mathcal{F}_{\theta^i}^i$ must be obtained at each iteration using the current parameters.

In multi-agent IRL, the set of policies, $\mathcal{F}_{\theta^i}^i(x_t)$, for k boundedly rational agents constitutes a (noisy) mixed-Nash solution obtained via backwards recursion through a set of Riccati equations [37] corresponding to the dynamic Gaussian game G if G is a linear-quadratic game with known linear dynamics and quadratic cost function. In unstructured crowds, however, the pedestrian dynamics are unknown. Recently, Scholler et al. [45] found that constant velocity motion models achieve state of the art results in motion planning tasks on pedestrian trajectory prediction benchmarks. Inspired by this result, we approximate the unknown systems dynamics with constant velocity dynamics,

$$\begin{bmatrix} \dot{p}^{i,x} \\ \dot{p}^{i,y} \\ \dot{\psi}^i \end{bmatrix} = \begin{bmatrix} 1 & 0 & 0 \\ 0 & 1 & 0 \\ 0 & 0 & 0 \end{bmatrix} \begin{bmatrix} v^{i,x} \\ v^{i,y} \\ 0 \end{bmatrix}, \quad (5)$$

Furthermore, as we do not know the cost functions \mathcal{J}^i , we approximate them via Taylor series expansion around the cumulative joint state value $\bar{x}_t = x_{1:t}$ to approximate \mathcal{J}^i as

$$\tilde{\mathcal{J}}^i(\bar{x} + \delta_{x_t}) \approx \tilde{\mathcal{J}}^i(\bar{x}) + \frac{1}{2} \delta_{x_t}^\top H_t^i \delta_{x_t} + l_t^{i\top} \delta_{x_t} \quad (6)$$

where $\delta_{x_t} = \bar{x}_t - x_t$ is the difference between the cumulative joint state and the joint state at the current time step. The matrix H_t^i and vector l_t^i correspond to the Hessian and gradient of the approximate cost function with respect to x_t . However, the constant velocity dynamics, combined with the fact that humans typically walk along linear paths at near identical speeds on average, results in a linear approximation of the cost function yielding a non-positive semidefinite H_t^i . This violates the assumptions made in Theorem 2 of [40] rendering the computation of \mathcal{F}_t^i intractable. More formally, Theorem 2 states that \mathcal{F}_t^i is a Gaussian distribution where the covariance matrix is obtained by computing $(H_t^i)^{-1}$, which is not defined for non-PSD matrices.

A solution to achieving tractability consists of modifying the assumption of bounded rationality. More formally, adding a constant factor to the diagonal elements of the learned covariance matrix makes inversion tractable at the cost of approximating the mixed-Nash equilibrium. As seen in our evaluation, this leads to a drop in accuracy in capturing the various behavior modes of individuals walking in a crowd.

B. Behavior Cloning [46], [41]

Given a set of expert demonstrations, behavior cloning (BC) aims to directly learn a policy in supervised learning fashion that maps states to actions. For pedestrian crowds, this involves learning how individuals navigate and interact in various scenarios. Expert demonstrations are collected as sequences of state-action pairs over a finite horizon T . Using the collected data, we train a model $F_{\theta^i}^i$ for each agent i to predict the expert’s action given a state. The objective is to minimize the difference between the predicted action and the expert’s action. Formally, the loss L for agent i is given by:

$$L(\theta^i) = \sum_{t=0}^T \left\| u_t^i - F_{\theta^i}^i(x_t^i) \right\|^2$$

where $\|\cdot\|$ denotes the Euclidean norm. Once the model is trained, it serves as the policy for the agent. For any given state x_t^i , the policy $F_{\theta^i}^i$ predicts the action u_t^i to be taken by the agent:

$$u_t^i = F_{\theta^i}^i(x_t^i)$$

While BC offers a direct approach to imitation learning, it’s essential to acknowledge its inherent limitations in the context of pedestrian crowds. First, BC is purely data-driven and the agent’s behavior is limited to the scope of the expert demonstrations. Small deviations, $\delta x_t^i = x_t^i - F_{\theta^i}^i(x_{t-1}^i)$, from the expert trajectory can therefore lead the agent into states not covered during training, resulting in unpredictable behavior, where δx_t^i represents the deviation at time t . This can be problematic in dynamic environments where

adaptability is crucial. Second, fewer expert trajectories could result in sub-optimal policies.

The choice of the representative algorithm for Behavior Cloning (BC) depends on the specific neural network architecture employed. For instance, the conventional baseline is the feed-forward neural network, often referred to as the multi-layer perceptron (MLP). Nevertheless, when it comes to capturing the temporal intricacies of trajectories, recurrent neural architectures like LSTMs prove to be a compelling option. Furthermore, the emergence of transformers has marked a significant impact on various computer vision and natural language processing benchmarks, making them another noteworthy candidate for a representative BC algorithm. In this study, we include all of these options as representative algorithms.

Hybrid IRL-BC. BC enables the imitation of expert demonstrations through a supervised learning paradigm. Despite its simplicity and practical results in allowing robots to generalize complex behaviors to new and unstructured scenarios [47], BC often suffers from compounding errors due to the fundamental design of the policy itself. In light of these challenges, we implement a novel hybrid model that synergizes the principles of Inverse Reinforcement Learning (IRL) and BC. This model is designed to uncover the underlying structures and “rewards” guiding expert behavior while preserving the practical and applicable nature of BC. In this innovative approach, we reformulate BC using implicit models, specifically, by employing the composition of $\arg \min$ with a continuous energy function E_θ to represent the policy π_θ as:

$$u_t^i = \arg \min_{u_t^i} E_\theta(x_t, u_t^i)$$

This reformulation allows the representation of policies implicitly and formulates imitation as a conditional Energy-Based Modeling (EBM) problem, optimizing actions by minimizing a continuous energy function conditioned on the observations. By integrating the inferred underlying structures of the expert’s behavior, akin to IRL, with the simplicity and direct applicability of BC, this model is considered as a hybrid IRL-BC approach.

C. Generative Models [42]

Generative models hold paramount importance in understanding and simulating potential behaviors in agents across multiple domains including computer vision and natural language processing. The overarching objective of these models is to learn and represent behaviors by discerning the underlying distributions and relationships between different states and actions. This is achieved by accurately estimating the parameters—means (μ) and covariances (Σ)—of fixed Gaussian components. Each Gaussian component in the model represents a potential behavior for the agent, symbolizing unique sets of actions associated with specific states, and is characterized by the probability density function:

$$P(x) = \frac{1}{\sqrt{(2\pi)^k |\Sigma|}} \exp\left(-\frac{1}{2}(x_t - \mu)^T \Sigma^{-1}(x_t - \mu)\right)$$

By learning the statistical properties embedded in these components, generative models are capable of producing actions and data points that are coherent with observed behaviors, thereby allowing for a comprehensive understanding

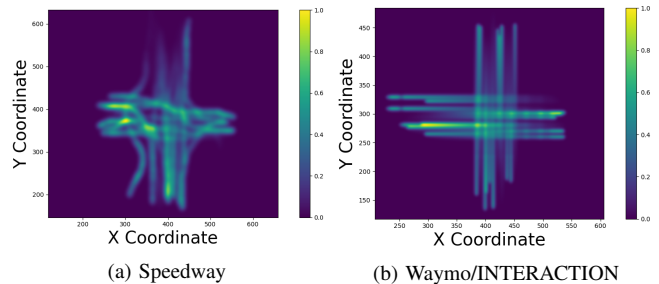


Fig. 3: Visualizing and comparing the entropy of trajectories in the Speedway dataset (1.061 bits) with the entropy of trajectories in the Waymo and INTERACTION datasets (0.336 and 0.475 bits, respectively). We observe that trajectories in the Speedway dataset are denser, more unstructured, and have a higher entropy, making it more suited for our analysis.

Dataset	Has SMGs?			
	Structured	Unstructured	Agents involved	Density (# agents / SMG)
SCAND [6]	✗	✗	-	-
JRDB [48]	✗	✗	-	-
Waymo [49]	✓(0.336 bits)	✗	Vehicles	2
INTERACTION [50]	✓(0.475 bits)	✗	Vehicles	2
Speedway	✗	✓(1.061 bits)	Pedestrians and Vehicles	2 – 4

TABLE I: Comparing of the Speedway dataset with state-of-the-art motion datasets: The Speedway dataset features trajectories of pedestrians as well as vehicles characterized by higher entropy (greater unpredictability) and increased density.

and representation of the variability and diversity inherent in agent actions. Once the model has adequately learned the means and covariances, it predicts actions by sampling from the established distributions using $u_t^i \sim \mathcal{N}(\mu, \Sigma)$, where u_t^i is the sampled action for i at time t representing a potential behavior of the agent, influenced by the learned parameters of the distribution. This meticulous process of learning and sampling provides profound insights into the plausible behaviors of agents, enabling the generation of actions that are not only consistent with observed data but also depict the intricate dependencies and variations among different states and actions. In essence, generative models serve as sophisticated tools for capturing and simulating the myriad of possible behaviors in agents by leveraging the relationships and distributions inherent in their actions and states.

V. EVALUATION AND DISCUSSION

We compare different IRL, generative, and BC approaches and aim to understand the following questions: *i)* How do different IL algorithms perform on real world SMGs and *(ii)* What are the current assumptions needed for successful IL in real world SMGs?

A. Speedway Dataset

We collected 3 hours of trajectory data at one of the busiest intersections (24th St. and Speedway) on The University of Texas at Austin campus using a Velodyne lidar mounted at the intersection. Our dataset consists primarily of tightly coupled agent interactions that are rarely found in existing autonomous driving and pedestrian datasets such as SCAND [6]. This type of data is useful for building safe and efficient decision-making and motion planning systems for robots in densely populated human environments such as homes, last mile delivery, and autonomous driving.

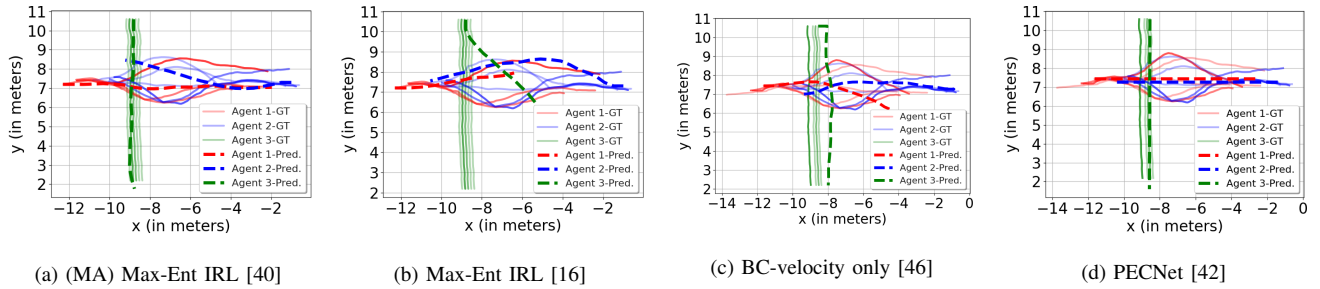


Fig. 4: **Qualitatively benchmarking imitation learning methods on the Speedway dataset**—Solid lines represent demonstration trajectories and dashed lines represent trajectories generated from the learned policies. The directions of movement for the agents are north to south (\downarrow), east to west (\leftarrow) and west to east (\rightarrow). ‘GT’ and ‘Pred’ refer to ground truth and predicted trajectories. *Conclusion:* Multi-agent (MA) MaxEnt IRL is most effective in capturing the behavior modes of the agents. MaxEnt IRL succeeds for at most one agent. Behavior cloning fails when tasked with predicting both the heading angle as well as the velocity, and predicts out of distribution trajectories.

The lidar continuously streams data as frames where each frame consists of the timestamp and a sequence of frame objects corresponding to agents observed by the lidar. Each frame object consists of a unique id that is persistent in all the frames in which the agent appears, location of the agent in meter with respect to its distance to the sensor, width and length of the bounding box detected for the agent, the angle of the detected bounding box in radian, the class type of the agent such as ‘pedestrian’ or ‘car’, the speed of the agents, and the accuracy of the detection. We recorded trajectories consisting of the id of the agents, their locations, speed, and orientation during busy moments (such as in between classes).

We processed the data by removing agents that were either at a standstill or appeared at the edges of the lidar’s field of view. Furthermore, we clipped each trajectory within a uniform spatio-temporal range ($[-20m, +20m]$ in the x axis and $[-10m, 15m]$ in the y axis). Each trajectory is finally processed in the form of a $T \times 4k$ array where T corresponds to the number of frames in that interaction and $4k$ corresponds to the dimension of the joint state, that is, $x_t = [p^i, v^i, \phi^i]^T$ for $i \in [1, k], p^i \in \mathbb{R}^2, v^i \in \mathbb{R}^1, \phi^i \in \mathbb{S}^1$. The final processed trajectories in the speedway dataset form the demonstration trajectories, denoted as \mathcal{D} . Features are computed based on distance to the goal position, distance to other agents, and control effort. For MaxEnt IRL and multi-agent MaxEnt IRL, since we do not know the true cost functions of the pedestrians, we directly minimize the root mean square error between the demonstration trajectories and the trajectories generated via the policy $\mathcal{F}_{\theta^i}^i$.

B. Baselines

BC-Transformer [46]—In the BC-Transformer baseline, we leverage the power of self-attention mechanisms. The state input consists of a 7-dimensional feature vector, similar to BC-LSTM. The transformer architecture comprises two encoder and decoder layers, each with 16 and 2 attention heads. To prevent overfitting, we apply a dropout rate of 0.2. Training utilizes the AdamW optimizer, with the loss function being Mean Squared Error (MSE). We set the learning rate to 3×10^{-4} and perform mini-batch training with a batch size of 64. A 60 – 40 cross-validation split is used for evaluation.

PECNet [42]—PECNet jointly predicts the trajectories of all

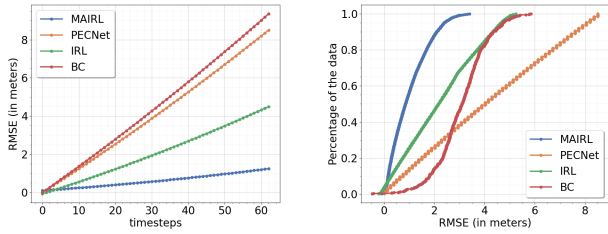
humans in a scene, while respecting social norms. An MLP network is first used to learn to predict sub-goal endpoints for each trajectory. This component encodes past trajectories and future endpoints to sample possible latent future endpoints. Next, the approach samples estimate of the endpoints from the previous step, coupled with a prediction network, to plan the future path using social pooling. This method was selected because of its state of the art performance on the ETH and UCY pedestrian motion planning benchmarks.

C. Benchmarking IL Methods on the Speedway Dataset

In this evaluation section, we present a comparison of BC, IRL, generative models, and a hybrid IRL-BC approach using the Speedway dataset. The evaluation focuses on their ability to learn policies for planning motion in complex scenarios involving tightly coupled human interactions. Figure 4 visually illustrates the comparisons, where solid lines represent demonstration trajectories and dashed lines represent trajectories generated from the learned cost functions, with arrows indicating the direction of movement. For clarity, we only show the results on the W-E-S dataset and defer the remaining results to the Appendix.

Multi-agent nature of IRL. Our findings demonstrate that multi-agent MaxEnt IRL outperforms MaxEnt IRL (Figures 4a and 4b), particularly when dealing with diverse trajectories from multiple agents. We further find that while multi-agent MaxEnt IRL outperforms MaxEnt IRL and BC in terms of matching the ground truth demonstrations (Figure 4), it still remains imperfect in capturing diverse behavior modes due to the constant identity covariance as discussed in Section III. Multi-agent MaxEnt IRL, in fact, does manage to capture the different behavior modes perfectly in simulation, as shown in Figure 6a, when the cost function takes a quadratic form. In the case of MaxEnt IRL, the collective cost function for three agents leads to suboptimal motion planning for the green agent, as observed by the green dashed line in Figure 4b. Moreover, MaxEnt IRL struggles to capture the motion of the westbound agent (red dashed line) in Figure 4b. MaxEnt IRL matches the ground truth demonstrations for 1 agent on average indicating that it will not scale to denser crowds.

BC, hybrid methods. Our findings reveal that Behavior Cloning (BC) and the hybrid BC-IRL approach generally encounter substantial difficulties, marked by their inability to



(a) Average RMSE per timestep. (b) Cumulative RMSE distribution.

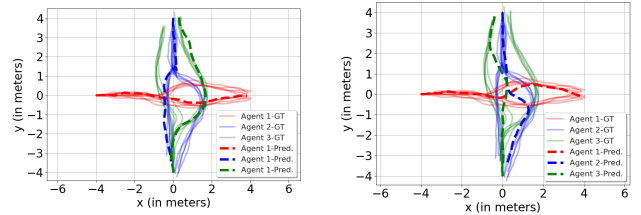
Fig. 5: Quantitatively benchmarking representative IL approaches: behavior cloning (BC [46]), inverse reinforcement learning (IRL [16] and MAIRL [40]), and generative methods (PECNet [42]). (left) Root mean square error per timestep; larger slope indicates poor long-term planning. (right) Cumulative RMSE distribution demonstrates the percentage of trajectories below a certain RMSE threshold; steeper curves indicate a more effective learner.

precisely encapsulate the behaviors of all three investigated agents. Particularly, the predictions generated by MaxEnt IRL reside relatively closer to the distribution of the ground truth demonstrations for specific agents, contrasting starkly with predictions from other examined methodologies, which exhibit considerable deviations—spanning several meters—from the groundtruth trajectories.

However, there exists a notable exception when the models are constrained to predict solely the velocity, provided that either the heading angle or an endpoint is supplemented as ground truth. As illustrated in Figure 4c, BC demonstrates commendable performance, even in a low data environment, when predicting only the velocity. Similarly, PECNet utilizes endpoint conditioning to forecast velocities exclusively. This revelation implies that the limitation of data does not categorically inhibit the feasibility of imitation learning for trajectory planning; rather, conditioning the learning task on supplementary state variables can serve as a valuable approach in such tightly coupled human interactions. These insights underscore the potential of employing strategically conditioned learning models as a viable alternative to navigate the challenges posed by scarce data availability, illuminating the prospects of more nuanced and adaptable learning methodologies in data-limited scenarios.

In Figure 5a, we quantitatively verify the qualitative results in the previous section. By measuring the root mean square error (RMSE) as a function of time, we observe that MAIRL incurs the lowest RMSE compared to BC, IRL, and PECNet, which implies that MAIRL most accurately recovers the ground truth reward functions of multiple agents, similar to Figure 4a. In Figure 5b, we measure the percentage of trajectories below a certain RMSE threshold; steeper curves indicate a more effective learner.

Simulation and Partial Conditioning. We hypothesize that the performance of imitation learning (IL) algorithms improves with access to global information. To validate this hypothesis, we conducted experiments running IL in both simulation and with partial conditioning (supplying training with partial state information). As shown in Figures 6a and 6b, the empirical observations suggest a direct correlation between the richness of information and the accuracy and efficacy of various IL algorithms. The results indicate that providing additional state information during training leads to improved



(a) Multi agent IRL

(b) Behavior cloning

Fig. 6: Simulation and Partial conditioning: We show that IL algorithms succeed when provided global information either in simulation (left) or via partial conditioning (right).

performance, validating our hypothesis and highlighting the importance of comprehensive state information in learning algorithms.

In summary, our evaluation reveals the following insights:

- Multi-agent cost function learning is important. Multi-agent MaxEnt IRL outperforms BC, MaxEnt IRL, generative models, and hybrid IRL-BC in terms of effectively learning policies for multiple agents with diverse behaviors.
- Conditioning on supplementary state variables or providing global information in simulation leads to better imitation learning.

VI. CONCLUSION

This research investigated the effectiveness of Imitation Learning (IL) techniques using a novel pedestrian dataset from the University of Texas at Austin campus. The key findings are as follows: (i) Multi-agent MaxEnt IRL outperformed BC, MaxEnt IRL, generative models, and hybrid IRL-BC in learning effective policies for multiple agents with diverse behaviors, highlighting the importance of multi-agent cost function learning in motion planning tasks in such scenarios. (ii) It was also observed that conditioning IL models on additional state variables improved their performance in low data regimes.

VII. FUTURE DIRECTIONS

The purpose of this study was to shed light on IL methods in real world social interaction scenarios. In light of the lessons learned through this work, several lines of future work emerge. First, given the observed success of multi-agent MaxEnt IRL in representing diverse behaviors in SMGs, future work should focus on developing strategies that model the multi-agent interactions, especially addressing challenges such as local observability. The promise shown by conditioning models on additional state variables suggests that investigating advanced conditioning strategies and integrating more sophisticated variables can significantly refine model predictions and improve outcomes. Real-world application and scalability of these models are also essential; testing and refining them in dynamic, real-world conditions such as malls or transit stations, and developing scalable solutions for denser crowds will be critical in assessing the reliability and applicability of these models. Lastly, incorporating external factors like weather and social contexts in modeling pedestrian behaviors can yield more holistic and precise predictions, providing a more comprehensive view of motion dynamics in various environments.

REFERENCES

- [1] R. Chandra, V. Zinage, E. Bakolas, P. Stone, and J. Biswas, “Deadlock-free, safe, and decentralized multi-robot navigation in social mini-games via discrete-time control barrier functions,” 2024.
- [2] R. Chandra, M. Wang, M. Schwager, and D. Manocha, “Game-theoretic planning for autonomous driving among risk-aware human drivers,” in *2022 International Conference on Robotics and Automation (ICRA)*, pp. 2876–2883, 2022.
- [3] R. Chandra and D. Manocha, “Gameplan: Game-theoretic multi-agent planning with human drivers at intersections, roundabouts, and merging,” *IEEE Robotics and Automation Letters*, vol. 7, no. 2, pp. 2676–2683, 2022.
- [4] N. Suriyarachchi, R. Chandra, J. S. Baras, and D. Manocha, “Gameopt: Optimal real-time multi-agent planning and control at dynamic intersections,” in *2022 IEEE 25th International Conference on Intelligent Transportation Systems (ITSC)*, pp. 2599–2606, IEEE doi - 10.1109/ITSC55140.2022.9921968, 2022.
- [5] A. Mavrogiannis, R. Chandra, and D. Manocha, “B-gap: Behavior-rich simulation and navigation for autonomous driving,” *IEEE Robotics and Automation Letters*, vol. 7, no. 2, pp. 4718–4725, 2022.
- [6] H. Karnan, A. Nair, X. Xiao, G. Warnell, S. Pirk, A. Toshev, J. Hart, J. Biswas, and P. Stone, “Socially compliant navigation dataset (scand): A large-scale dataset of demonstrations for social navigation,” *IEEE Robotics and Automation Letters*, vol. 7, no. 4, pp. 11807–11814, 2022.
- [7] A. H. Raj, Z. Hu, H. Karnan, R. Chandra, A. Payandeh, L. Mao, P. Stone, J. Biswas, and X. Xiao, “Targeted learning: A hybrid approach to social robot navigation,” 2023.
- [8] Z. Sprague, R. Chandra, J. Holtz, and J. Biswas, “Socialgym 2.0: Simulator for multi-agent social robot navigation in shared human spaces,” *arXiv preprint arXiv:2303.05584*, 2023.
- [9] R. Chandra, R. Maligi, A. Anantula, and J. Biswas, “Socialmapf: Optimal and efficient multi-agent path finding with strategic agents for social navigation,” *IEEE Robotics and Automation Letters*, 2023.
- [10] R. Chandra, R. Menon, Z. Sprague, A. Anantula, and J. Biswas, “Decentralized social navigation with non-cooperative robots via bi-level optimization,” *arXiv preprint arXiv:2306.08815*, 2023.
- [11] R. Chandra, V. Zinage, E. Bakolas, J. Biswas, and P. Stone, “Decentralized multi-robot social navigation in constrained environments via game-theoretic control barrier functions,” *arXiv preprint arXiv:2308.10966*, 2023.
- [12] S. Poddar, C. Mavrogiannis, and S. S. Srinivasa, “From crowd motion prediction to robot navigation in crowds,” 2023.
- [13] A. Francis, C. Pérez-D’Arpino, C. Li, F. Xia, A. Alahi, R. Alami, A. Bera, A. Biswas, J. Biswas, R. Chandra, H.-T. L. Chiang, M. Everett, S. Ha, J. Hart, J. P. How, H. Karnan, T.-W. E. Lee, L. J. Manso, R. Mirksy, S. Pirk, P. T. Singamaneni, P. Stone, A. V. Taylor, P. Trautman, N. Tsoi, M. Vázquez, X. Xiao, P. Xu, N. Yokoyama, A. Toshev, and R. Martín-Martín, “Principles and guidelines for evaluating social robot navigation algorithms,” 2023.
- [14] F. Torabi, G. Warnell, and P. Stone, “Recent advances in imitation learning from observation,” *arXiv preprint arXiv:1905.13566*, 2019.
- [15] B. Zheng, S. Verma, J. Zhou, I. W. Tsang, and F. Chen, “Imitation learning: Progress, taxonomies and challenges,” *IEEE Transactions on Neural Networks and Learning Systems*, no. 99, pp. 1–16, 2022.
- [16] B. D. Ziebart, A. L. Maas, J. A. Bagnell, A. K. Dey, et al., “Maximum entropy inverse reinforcement learning,” in *Aaai*, vol. 8, pp. 1433–1438, Chicago, IL, USA, 2008.
- [17] M. Bain and C. Sammut, “A framework for behavioural cloning,” in *Machine Intelligence 15*, 1995.
- [18] S. Ross, G. J. Gordon, and J. A. Bagnell, “A reduction of imitation learning and structured prediction to no-regret online learning,” 2011.
- [19] S. Daffry, J. A. Bagnell, and M. Hebert, “Learning transferable policies for monocular reactive mav control,” 2016.
- [20] P. Sermanet, C. Lynch, Y. Chebotar, J. Hsu, E. Jang, and S. Levine, “Time-contrastive networks: Self-supervised learning from video,” 2018.
- [21] N. Ratliff, D. Bradley, J. A. Bagnell, and J. Chestnutt, “Boosting structured prediction for imitation learning,” in *Proceedings of the 19th International Conference on Neural Information Processing Systems, NIPS’06*, (Cambridge, MA, USA), pp. 1153–1160, MIT Press, 2006.
- [22] C. L. Baker, R. Saxe, and J. Tenenbaum, “Action understanding as inverse planning,” *Cognition*, vol. 113, pp. 329–349, 2009.
- [23] R. S. Sutton and A. G. Barto, *Reinforcement Learning: An Introduction*. MIT Press, 2018.
- [24] J. Ho and S. Ermon, “Generative adversarial imitation learning,” in *Proceedings of the 30th International Conference on Neural Information Processing Systems*, pp. 4572–4580, 2016.
- [25] I. Kostrikov, O. Nachum, and J. Tompson, “Imitation learning via off-policy distribution matching,” 2019.
- [26] R. Dadashi, L. Hussenot, M. Geist, and O. Pietquin, “Primal wasserstein imitation learning,” *CoRR*, vol. abs/2006.04678, 2020.
- [27] P. Abbeel and A. Y. Ng, “Apprenticeship learning via inverse reinforcement learning,” in *Proceedings of the twenty-first international conference on Machine learning*, p. 1, 2004.
- [28] A. Alahi, K. Goel, V. Ramanathan, A. Robicquet, L. Fei-Fei, and S. Savarese, “Social lstm: Human trajectory prediction in crowded spaces,” in *Proceedings of the IEEE conference on computer vision and pattern recognition*, pp. 961–971, 2016.
- [29] S. Ross, G. J. Gordon, and J. A. Bagnell, “A reduction of imitation learning and structured prediction to no-regret online learning,” 2011.
- [30] S. Levine and V. Koltun, “Continuous inverse optimal control with locally optimal examples,” *arXiv preprint arXiv:1206.4617*, 2012.
- [31] C. Finn, S. Levine, and P. Abbeel, “Guided cost learning: Deep inverse optimal control via policy optimization,” in *Proceedings of the International Conference on Machine Learning*, pp. 49–58, 2016.
- [32] S. A. et al., “Imitating human reaching motions using physically inspired optimization principles,” in *Proceedings of the 11th IEEE-RAS International Conference on Humanoid Robots*, pp. 602–607, 2011.
- [33] K. Mombaur, A. T. Truong, and J.-P. Laumond, “From human to humanoid locomotion—an inverse optimal control approach,” *Autonomous Robots*, vol. 28, no. 3, pp. 369–383, 2010.
- [34] L. Yu, J. Song, and S. Ermon, “Multi-agent adversarial inverse reinforcement learning,” in *International Conference on Machine Learning*, pp. 7194–7201, PMLR, 2019.
- [35] J. Song, H. Ren, D. Sadigh, and S. Ermon, “Multi-agent generative adversarial imitation learning,” *Advances in neural information processing systems*, vol. 31, 2018.
- [36] W. Schwarting, A. Pierson, J. Alonso-Mora, S. Karaman, and D. Rus, “Social behavior for autonomous vehicles,” *Proc. Nat. Acad. Sci.*, vol. 116, no. 50, pp. 24972–24978, 2019.
- [37] S. Lecleac’h, M. Schwager, and Z. Manchester, “Lucidgames: Online unscented inverse dynamic games for adaptive trajectory prediction and planning,” *IEEE Robot. Automat. Lett.*, vol. 6, pp. 5485–5492, Jul. 2021.
- [38] S. Rothfuß, J. Inga, F. Köpf, M. Flad, and S. Hohmann, “Inverse optimal control for identification in non-cooperative differential games,” in *IFAC-PapersOnLine*, vol. 50, pp. 14909–14915, 2017.
- [39] F. Köpf, J. Inga, S. Rothfuß, M. Flad, and S. Hohmann, “Inverse reinforcement learning for identification in linear-quadratic dynamic games,” in *IFAC-PapersOnLine*, vol. 50, pp. 14902–14908, 2017.
- [40] N. Mehr, M. Wang, M. Bhatt, and M. Schwager, “Maximum-entropy multi-agent dynamic games: Forward and inverse solutions,” *IEEE Transactions on Robotics*, 2023.
- [41] F. Torabi, G. Warnell, and P. Stone, “Behavioral cloning from observation,” *arXiv preprint arXiv:1805.01954*, 2018.
- [42] K. Mangalam, H. Girase, S. Agarwal, K.-H. Lee, E. Adeli, J. Malik, and A. Gaidon, “It is not the journey but the destination: Endpoint conditioned trajectory prediction,” in *Computer Vision—ECCV 2020: 16th European Conference, Glasgow, UK, August 23–28, 2020, Proceedings, Part II 16*, pp. 759–776, Springer, 2020.
- [43] D. Gonon and A. Billard, “Inverse reinforcement learning of pedestrian–robot coordination,” *IEEE Robotics and Automation Letters*, 2023.
- [44] S. J. Wright, “Coordinate descent algorithms,” *Mathematical programming*, vol. 151, no. 1, pp. 3–34, 2015.
- [45] C. Schöller, V. Aravantinos, F. Lay, and A. Knoll, “What the constant velocity model can teach us about pedestrian motion prediction,” *IEEE Robotics and Automation Letters*, vol. 5, no. 2, pp. 1696–1703, 2020.
- [46] F. Giuliani, I. Hasan, M. Cristani, and F. Galasso, “Transformer networks for trajectory forecasting,” in *2020 25th international conference on pattern recognition (ICPR)*, pp. 10335–10342, IEEE, 2021.
- [47] X. Xiao, Z. Xu, Z. Wang, Y. Song, G. Warnell, P. Stone, T. Zhang, S. Ravi, G. Wang, H. Karnan, J. Biswas, N. Mohammad, L. Bramblett, R. Peddi, N. Bezzo, Z. Xie, and P. Dames, “Autonomous ground navigation in highly constrained spaces: Lessons learned from the barn challenge at icra 2022,” 2022.
- [48] R. Martin-Martin, M. Patel, H. Rezatofighi, A. Sheno, J. Gwak, E. Frankel, A. Sadeghian, and S. Savarese, “Jrdb: A dataset and benchmark of egocentric robot visual perception of humans in built environments,” *IEEE transactions on pattern analysis and machine intelligence*, vol. 45, no. 6, pp. 6748–6765, 2021.
- [49] S. Eittinger, S. Cheng, B. Caine, C. Liu, H. Zhao, S. Pradhan, Y. Chai, B. Sapp, C. R. Qi, Y. Zhou, et al., “Large scale interactive motion forecasting for autonomous driving: The waymo open motion dataset,” in *Proceedings of the IEEE/CVF International Conference on Computer Vision*, pp. 9710–9719, 2021.
- [50] W. Zhan, L. Sun, D. Wang, H. Shi, A. Clausse, M. Naumann, J. Kummerle, H. Königshof, C. Stiller, A. de La Fortelle, et al., “Interaction dataset: An international, adversarial and cooperative motion dataset in interactive driving scenarios with semantic maps,” *arXiv preprint arXiv:1910.03088*, 2019.